

RESEARCH ARTICLE

A Novel Dual-Band Printed Monopole Antenna With Modified SIR Loading

HONGLIN ZHANG¹, TENG SUN¹, WENCHENG REN¹, CHUNLEI YUAN¹, AND DONG CHEN^{2,3}¹54th Research Institute of China Electronic Technology Group Corporation (CETC54), Shijiazhuang, Hebei 050081, China²College of Electronic and Optical Engineering, Nanjing University of Posts and Telecommunications, Nanjing, Jiangsu 050081, China³College of Flexible Electronics, Nanjing University of Posts and Telecommunications, Nanjing, Jiangsu 050081, China

Corresponding author: Honglin Zhang (zhlandhsl@163.com)

ABSTRACT In this paper, a novel dual-band compact printed monopole antenna is presented. The antenna is composed of three spatially distributed layers: a modified folded-line stepped impedance resonator (SIR) on the upper layer, a printed monopole antenna on the middle layer, and another folded-line SIR on the lower layer. A pair of resonant frequencies can be introduced by loading two different modified folded-line SIRs as near-field resonant parasitic elements (NFRPs) in the near field of a printed monopole antenna. Simultaneously, the resonant frequencies of the two are lower than the fundamental mode frequency of a traditional printed monopole antenna, thereby enabling the realization of a compact antenna. Furthermore, the resonant frequency can be adjusted through the wide edge strong coupling between the folded-line SIR and the printed monopole antenna. After elaborating on the design principles, a sample antenna is fabricated and underwent measurements to validate the anticipated performance of the proposed antenna. The measured outcomes closely align with the predicted results, providing compelling evidence that the design methodology expounded in this paper is indeed precise and efficacious.

INDEX TERMS Dual-band, modified folded-line SIR, compact, near-field, loading.

I. INTRODUCTION

Due to the rapid development of wireless communication systems, the printed monopole antenna has become a crucial component in wireless applications. Therefore, it is necessary to fabricate an antenna capable of operating in two distinct frequency bands in order to meet the demands of personal wireless communication users who require multi-band standard services. Several variations of dual-band printed monopole antennas have been documented, such as those that utilize tilted-D-shaped strips [1], two different sizes of stacked T-shaped loading [2], split-ring element loading [3], and printed double meander line [4] and so on. Nonetheless, in practical applications, the majority of such designs have significant dimensions or complex structures.

Recently, a multitude of compact printed monopole antennas have been developed and designed. In [5], the dual-band antenna is implemented using CPW feeding. In [6], the

antenna achieves dual-band operation through loading a strip-sleeve structure. In [7], two different monopole branches are employed to generate two resonance frequencies. Reference [8] proposes a compact dual-band antenna with two folded strips for enhanced performance.

In recent times, the concept of near-field resonant parasitic (NFRP) has emerged as a unique design pathway for dual-band antenna. In [9], a dual-band monopole antenna was introduced with NFRP in the form of Z-shaped meander lines. Reference [10] has shown that a tri-band monopole antenna can be created through the utilization of NFRP elements such as one meander line dipole and two arrow-type dipoles. Reference [11] introduced a dual-band monopole antenna consisting of two capacitively-loaded loop (CLL) NFRP elements. In [12], the dual-band properties of the antenna were realized through the utilization of Egyptian axe NFPR elements.

This paper presents a compact printed dual-band monopole antenna with modified folded-line SIR loading. Two resonance frequencies are introduced as a result of the coupling

The associate editor coordinating the review of this manuscript and approving it for publication was Bilal Khawaja¹.

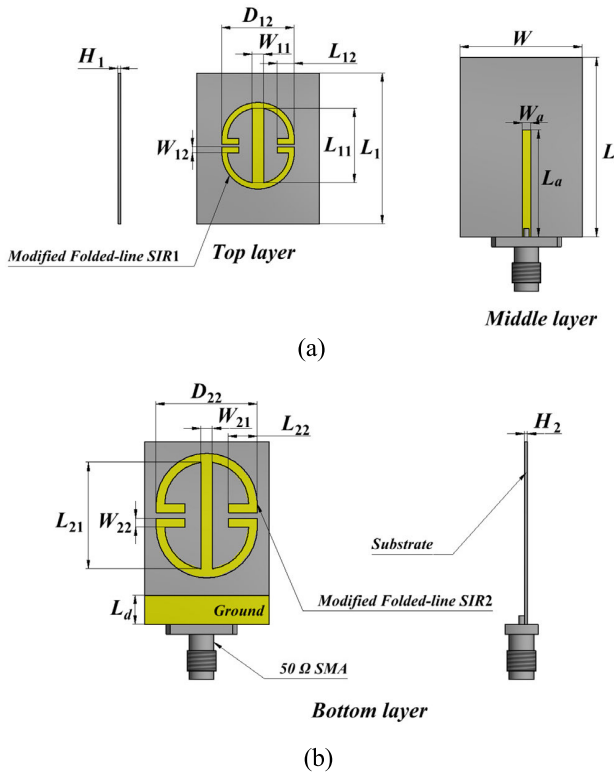


FIGURE 1. Physical layout of the proposed printed compact monopole antenna. (a) Top layer and Middle layer (b) Bottom layer.

between the modified folded-line SIR element as NFRP elements and the printed monopole antenna. Simultaneously, when compared to traditional printed monopole antennas, loading an NFRP element reduces the resonant frequency, enabling a more compact antenna design. After conducting a thorough analysis of the principles outlined in this paper, a sample antenna was fabricated and measurement. The resulting measurements align well with the anticipated outcomes.

II. ANTENNA DESIGN

A. ANTENNA CONFIGURATION

The structure of the proposed compact printed monopole dual-band antenna is presented in Fig.1. The proposed antenna comprises of a printed monopole that serves as the driving element, along with two different SIRs are printed on both the top and bottom layers of the substrate, respectively. Positioned in the middle layer of the substrate is the driving printed monopole. As shown in Fig. 1, W_{11} , W_{21} , L_{11} , and L_{12} are the dimensions for modifying the folded SIR1, while W_{21} , W_{22} , L_{21} , and L_{22} are the dimensions for modifying the folded SIR2. The thickness of the top layer substrate is H_1 , and the bottom layer substrate is H_2 . The overall dimensions of the antenna are L and W . The size parameters are shown in Table 1.

The entire antenna is connected to a 50-ohm SMA connector through a microstrip line. All structure of the antenna

TABLE 1. Geometric parameters of the proposed printed monopole antenna.

Parameter	Value(mm)	Parameter	Value(mm)
W	21.4	L_{12}	2.6
W_{11}	2.0	L_{21}	18.1
W_{12}	1.0	L_{22}	4.6
W_{21}	1.8	D_{12}	13.6
W_{22}	0.8	D_{22}	17.2
W_a	1.2	L_a	17.9
L	29.8	L_d	5.0
L_1	24.8	H_1	0.508
L_{11}	13.9	H_2	0.508

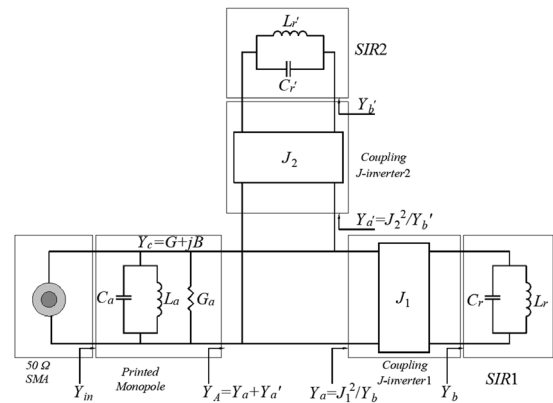


FIGURE 2. Equivalent circuit of the proposed dual-band compact monopole antenna.

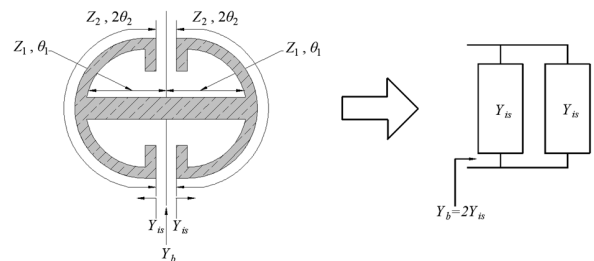


FIGURE 3. Modified folded-line SIR and its equivalent circuit.

are printed on a substrate of Rogers RO4003C with relative dielectric constant $\epsilon_r = 3.38$ and the loss tangent $\tan\delta = 0.0027$, respectively.

B. DESIGN OF THE PROPOSED ANTENNA

The mechanism of the proposed compact dual-band printed monopole antenna is to introduce two different resonant modes by loading two different SIRs as NFRP elements in the near field of the antenna [13]. In order to comprehend the mechanism of the proposed compact dual-band printed monopole antenna, an equivalent circuit as shown in Fig. 2 was adopted.

In our design, there are two different modified folded-line SIRs that serve as NFRP elements. In order to simplify analysis, the modified folded-line SIR1 (SIR2 has a similar structure to SIR1) was analyzed. The modified folded-line SIR and its equivalent circuit are shown in Fig. 3. The modified folded-line SIR can be seen as two parallel basic SIRs, and its equivalent circuit is composed of two admittances, which are represented as Y_{is} . Y_{is} is as follows [14].

$$Y_{is} = j \frac{2Z_2 \tan \theta_1 + Z_1 \tan \theta_2}{Z_1(2Z_2 - Z_1 \tan \theta_1 \times \tan \theta_2)} \quad (1)$$

where, Z_1 and Z_2 are the characteristic impedance of the microstrip line, while θ_1 and θ_2 are the electrical lengths of the microstrip line, respectively.

As can be seen from Fig. 3, Y_b can be obtained from a couple of shunt admittance Y_{is} .

$$Y_b = 2Y_{is} = j \frac{4Z_2 \tan \theta_1 + 2Z_1 \tan \theta_2}{Z_1(2Z_2 - Z_1 \tan \theta_1 \times \tan \theta_2)} \quad (2)$$

In the same way, it is possible to obtain Y'_b

$$Y'_b = j \frac{4Z'_2 \tan \theta'_1 + 2Z'_1 \tan \theta'_2}{Z'_1(2Z'_2 - Z'_1 \tan \theta'_1 \times \tan \theta'_2)} \quad (3)$$

Where, Z'_1 , Z'_2 , θ'_1 , and θ'_2 are the characteristic impedances and electrical lengths, respectively.

Based on the fundamental understanding of parallel coupled filter design cited in [15], the coupling of the printed monopole and SIR can be described as a J-inverter.

The folded-line SIR can be equivalently represented as a lossless parallel LC circuit, denoted by L_r and C_r .

According to the application of the J-inverter [16], the admittance relation can be established

$$Y_a = J_1^2/Y_b = j \frac{J_1^2 Z_1 (2Z_2 - Z_1 \tan \theta_1 \times \tan \theta_2)}{4Z_2 \tan \theta_1 + 2Z_1 \tan \theta_2} \quad (4)$$

Similarly, Y'_a can be obtained

$$Y'_a = J_2^2/Y'_b = j \frac{J_2^2 Z'_1 (2Z'_2 - Z'_1 \tan \theta'_1 \times \tan \theta'_2)}{4Z'_2 \tan \theta'_1 + 2Z'_1 \tan \theta'_2} \quad (5)$$

From the shunt admittance Y_a and Y'_a , Y_A is as follows

$$Y_A = Y_a + Y'_a = j \left[\frac{J_2^2 Z'_1 (2Z'_2 - Z'_1 \tan \theta'_1 \times \tan \theta'_2)}{4Z'_2 \tan \theta'_1 + 2Z'_1 \tan \theta'_2} + \frac{J_1^2 Z_1 (2Z_2 - Z_1 \tan \theta_1 \times \tan \theta_2)}{4Z_2 \tan \theta_1 + 2Z_1 \tan \theta_2} \right] \quad (6)$$

The admittance Y_c of the printed monopole is

$$Y_c = G_c + jB_c \quad (7)$$

where, G_c and B_c represent the real part and the imaginary part of admittance Y_c , respectively. Ultimately,

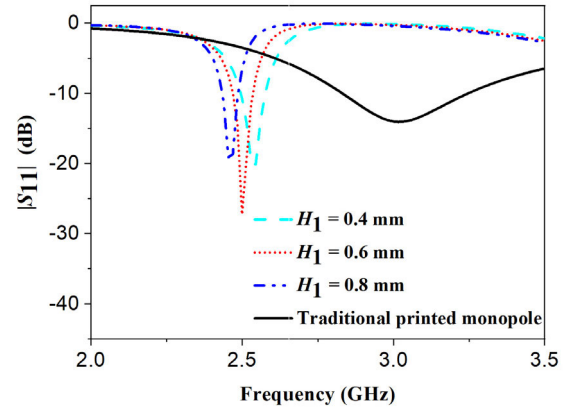


FIGURE 4. The simulated S_{11} varies with H_1 (without modified the folded-line SIR2).

input admittance Y_{in} can be obtained,

$$Y_{in} = Y_A + Y_c = G_c + j \left[B_c + \frac{J_1^2 Z_1 (2Z_2 - Z_1 \tan \theta_1 \times \tan \theta_2)}{4Z_2 \tan \theta_1 + 2Z_1 \tan \theta_2} + \frac{J_2^2 Z'_1 (2Z'_2 - Z'_1 \tan \theta'_1 \times \tan \theta'_2)}{4Z'_2 \tan \theta'_1 + 2Z'_1 \tan \theta'_2} \right] \quad (8)$$

Based on formula (8), it is evident that the input admittance Y_{in} changes with the J-inverter when the printed monopole and folded-line SIRs are determined. However, according to [17], the coupling between printed monopoles and folded-line SIR is determined by the distance between them, which is also equivalent to the J-inverter. As a result, the values of J_1 and J_2 are depicted in Fig.2 can be determined by the physical dimensions of H_1 and H_2 shown in Fig.1. Subsequently, the parameters of the proposed antenna were simulated and analyzed using the CST STUDIO SUITE software.

When the modified folded-line SIR1 is used alone (without the SIR2) is employed, Fig.4 shows the simulated changes in reflection coefficients as H_1 varies. In the simulation, the other dimensional parameters remain as shown in Table 1.

As shown in Fig.4, the frequency at which the antenna resonates gradually decreases as the value of H_1 increases. In other words, as the broadside distance between the printed monopole antenna and the modified folded-line SIR1 increases, the coupling decreases, causing the resonant frequency of the antenna to decrease. Also, Fig. 4 depicts the reflection coefficient of the traditional printed monopole antenna. In comparison to the reflection coefficient of the traditional printed monopole antenna, the resonant frequency of the antenna with modified folded-line SIR1 loading is notably decreased.

Afterwards, both modified folded-lines SIR1 and SIR2 are loaded simultaneously. To demonstrate this phenomenon in a step-by-step manner, the simulation initially focuses on the variation of echo loss with H_1 while holding H_2 constant, as depicted in Fig.5. In the simulation, the other dimensional parameters remain as shown in Table 1.

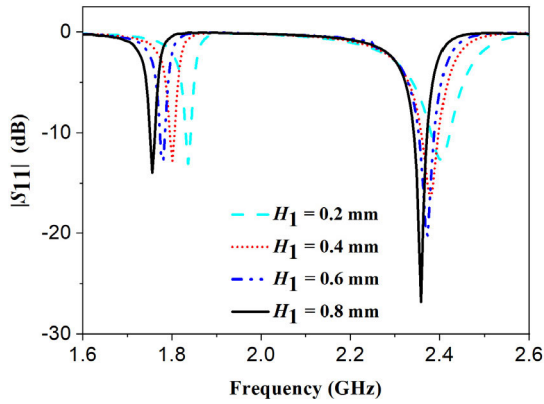


FIGURE 5. The simulated S_{11} varies with H_1 (H_2 is fixed).

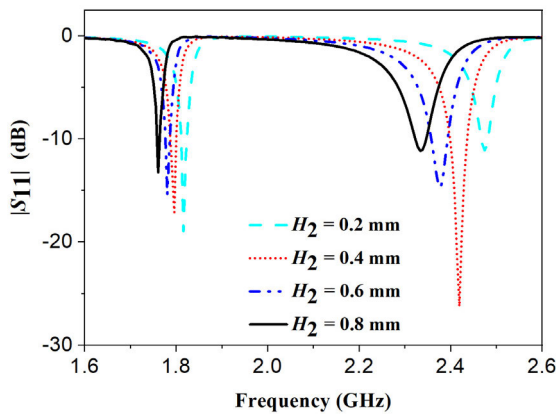


FIGURE 6. The simulated S_{11} varies with H_2 (H_1 is fixed).

Fig.5 shows that the antenna has a dual-band feature. As explained earlier, the modified folded-line SIR1 has its resonant frequency in the higher frequency band on the right side, while the modified folded-line SIR2 has its resonant frequency in the lower frequency band on the left side. From Fig. 5, it can be observed that the resonance frequency of the modified folded-line SIR1 decreases as H_1 increases. This implies that the resonance frequency increases with the coupling between the modified folded-line SIR1 and the printed monopole is enhanced.

The reflection coefficient at different H_2 values (with H_1 held constant) is presented in Fig.6, which further visualizes the aforementioned phenomenon. In the simulation, the other dimensional parameters remain as shown in Table 1.

Meanwhile, $H_1 = H_2$ is defined. As shown in Fig.7, the reflection coefficient varies with the changes in H_1 and H_2 . And as H_1 and H_2 decrease, the two resonant frequencies gradually decrease. In the simulation, the other dimensional parameters remain as shown in Table 1.

III. MEASURED RESULTS

A sample antenna is manufactured and measured to verify our design. The dimensions have been optimized through the use of CST electromagnetic simulation software, as indicated in

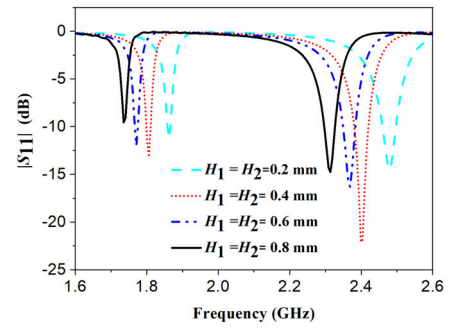


FIGURE 7. The simulated S_{11} varies with H_1 and H_2 ($H_1 = H_2$).



FIGURE 8. Photograph of the proposed printed monopole antenna.

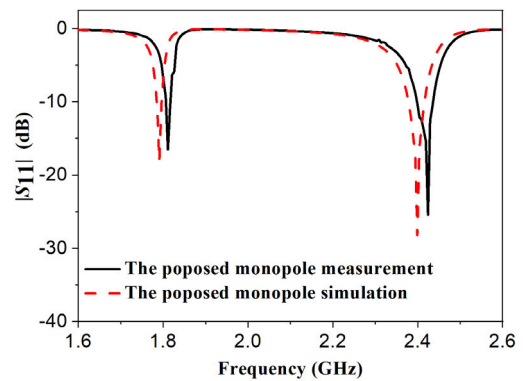
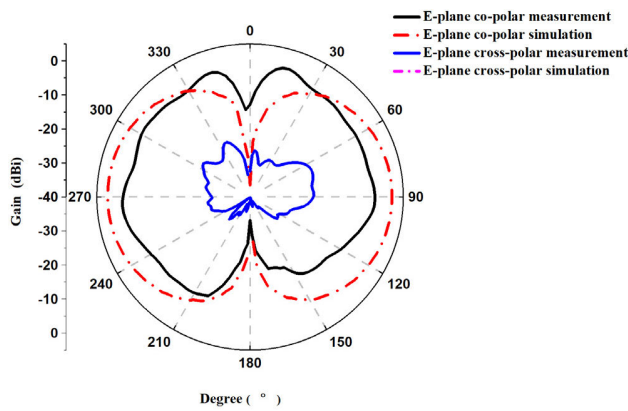


FIGURE 9. Simulated and measured return loss of the antenna.

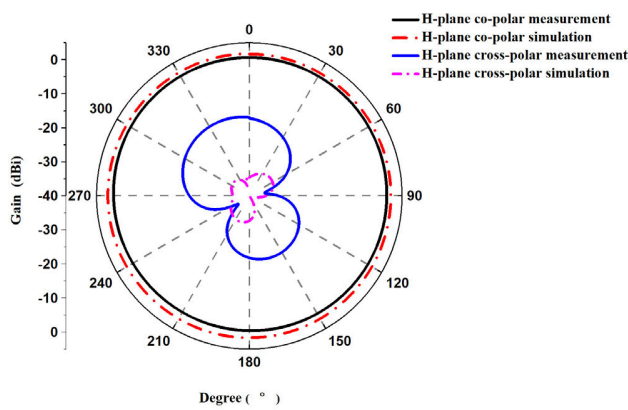
Table 1. In Fig. 8, a physical photo of the proposed antenna is presented. The reflection coefficient of the antenna was measured using the Keysight E5071C vector network analyzer, and the radiation pattern of the antenna was measured using the SATIMO near-field antenna measurement system.

Fig.9 illustrates a comparative analysis between simulated and measured reflection coefficients. It can be seen from Fig.9 that the simulation and test results are very consistent.

Fig.10 and Fig.11 respectively depict the radiation pattern of the proposed antenna in the E-plane and H-plane at frequencies of 1.81GHz and 2.42GHz. It is evident that the



(a)



(b)

FIGURE 10. Simulated and measured radiation patterns of the proposed monopole antenna at 1.81 GHz. (a) E plane (b) H plane.

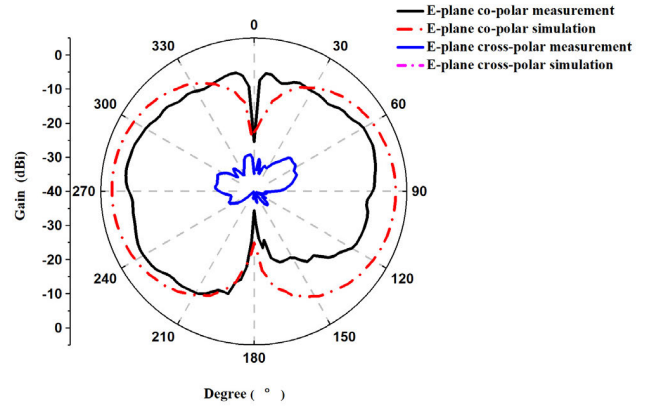
proposed antenna exhibits impressive omnidirectional radiation characteristics and low levels of cross-polarization.

Fig. 12 depicts the simulated and measured gain of the proposed compact monopole antenna. As can be seen from the results, the antenna achieves a stable gain over the operating frequency range. At the same time, it can be seen from Fig. 12 that there are two gain peaks, 1.82dBi and 2.35 dBi, which are in good agreement with the simulation results.

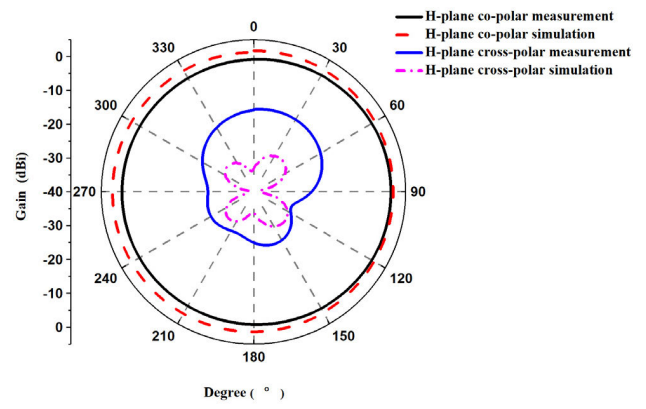
Similarly, Fig. 13 shows the comparison curves of the proposed printed monopole antenna simulation and measured radiation efficiency in the operating frequency range. In Fig. 13, there are two peaks on the measured radiation efficiency curve, with 83% and 87%, respectively.

It is important to note that gain and efficiency are often low at high frequency. This may be due to an increase in metal losses at high frequencies. Similarly, the slight deviation between the simulation and measurement may be caused by the variation of the welding precision of SMA and the dielectric constant of the substrate.

A comparison of the proposed dual-band printed monopole antenna with the other published references in recent years is shown in Table 2.



(a)



(b)

FIGURE 11. Simulated and measured radiation patterns of the proposed monopole antenna at 2.42 GHz. (a) E plane (b) H plane.

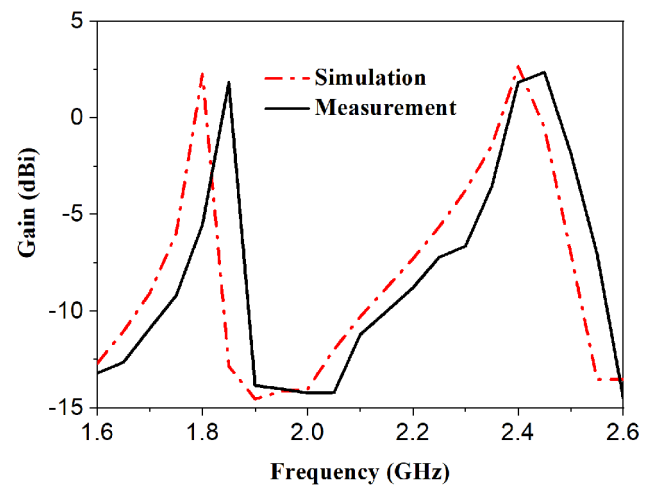


FIGURE 12. Simulated and measured radiation gain of the proposed printed monopole antenna.

The proposed dual-band compact printed monopole antenna has better performance in terms of gain and return loss, respectively, compared with other antennas listed in Table 2. Compared with the other antennas in Table 2, the

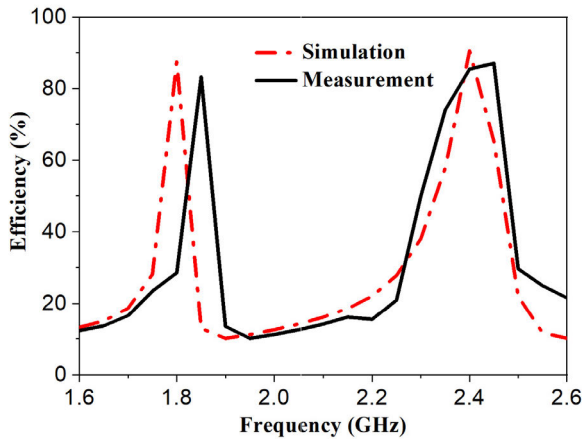


FIGURE 13. Simulated and measured radiation efficiency of the proposed printed monopole antenna.

TABLE 2. Comparison of various dual-band printed monopole antenna.

Ref.	Freq. (GHz)	Size (mm)	Gain (dBi)	S ₁₁ (dB)
18	1.8/2.45	51×41.5×82	0.5/1.5	-16.5/-12.1
19	1.8/2.4	60×100×4.1	1.5/0.5	-15.5/-32.5
20	1.8/2.4	54×46×15	N/A	-18.5/-19.4
21	1.8/2.8	65×75×0.705	2/0.63	-28/-15
The proposed antenna	1.81/2.42	21.4×29.8×1.016	1.82/2.35	-21.5/-26.4

proposed dual-band compact printed monopole antenna has relatively small physical dimensions.

IV. CONCLUSION

This paper introduces a novel compact dual-band monopole antenna that utilizes modified folded-line SIR loading. By loading a pair of modified folded-line SIRs as NFRP element, the dual-band characteristics of the antenna can be achieved. Due to that fact that two folded-line SIRs are loaded at the top and bottom of the printed monopole antenna, the overall size of the antenna does not increase, thus enabling a compact antenna design. The simulation results demonstrate a high level of consistency with the actual measurement. In the meantime, the proposed antenna exhibits an omnidirectional radiation pattern, thereby offering substantial confirmation for the proposed design methodology.

REFERENCES

[1] A. Altaf and M. Seo, "A tilted-D-shaped monopole antenna with wide dual-band dual-sense circular polarization," *IEEE Antennas Wireless Propag. Lett.*, vol. 17, pp. 2464–2468, 2018.

[2] Y.-L. Kuo and K.-L. Wong, "Printed double-T monopole antenna for 2.4/5.2 GHz dual-band WLAN operations," *IEEE Trans. Antennas Propag.*, vol. 51, no. 9, pp. 2187–2192, Sep. 2003.

[3] T. Yue, Z. H. Jiang, and D. H. Werner, "A compact metasurface-enabled dual-band dual-circularly polarized antenna loaded with complementary split ring resonators," *IEEE Trans. Antennas Propag.*, vol. 67, no. 2, pp. 794–803, Feb. 2019.

[4] Z.-X. Xia, K. W. Leung, M. W. K. Lee, and N. Yang, "Miniature dual-band meander-line monopole chip antenna with independent band control," *IEEE Antennas Wireless Propag. Lett.*, vol. 18, pp. 1873–1877, 2019.

[5] H.-D. Chen and H.-T. Chen, "A CPW-fed dual-frequency monopole antenna," *IEEE Trans. Antennas Propag.*, vol. 52, no. 4, pp. 978–982, Apr. 2004.

[6] C. H. Cheng, W. J. Lv, Y. Chen, and H. B. Zhu, "A dual-band strip-sleeve monopole antenna fed by CPW," *Microw. Opt. Technol. Lett.*, vol. 42, no. 1, pp. 70–73, Jul. 2004.

[7] M. N. Suma, R. K. Raj, M. Joseph, P. C. Bybi, and P. Mohanan, "A compact dual band planar branched monopole antenna for DCS/2.4-GHz WLAN applications," *IEEE Microw. Wireless Compon. Lett.*, vol. 16, no. 5, pp. 275–277, May 2006.

[8] W.-C. Liu and P.-C. Kao, "Compact CPW-fed dual folded-strip monopole antenna for 5.8-GHz RFID application," *Microw. Opt. Technol. Lett.*, vol. 48, no. 8, pp. 1614–1615, Aug. 2006.

[9] P. Jin and R. W. Ziolkowski, "Multiband extensions of the electrically small, near-field resonant parasitic Z antenna," *IET Microw., Antennas Propag.*, vol. 4, no. 8, pp. 1016–1025, Aug. 2010.

[10] C.-C. Lin, R. W. Ziolkowski, and P. Jin, "A compact planar near field resonant parasitic (NFRP) antenna for MIMO applications," in *Proc. IEEE Int. Symp. Antennas Propag. (APSURSI)*, Jul. 2011, pp. 167–170.

[11] R. W. Ziolkowski, P. Jin, and C.-C. Lin, "Metamaterial-inspired, multi-functional, near-field resonant parasitic antennas," in *Proc. IEEE Int. Conf. Wireless Inf. Technol. Syst.*, Aug. 2010, pp. 1–4.

[12] R. W. Ziolkowski, P. Jin, and C.-C. Lin, "Planar, multi-band, linear and circular polarized, electrically small, near field resonant parasitic antennas and their smart dust applications," in *Proc. Int. Workshop Antenna Technol. (IWAT)*, Mar. 2011, pp. 21–24.

[13] R. W. Ziolkowski, "Efficient electrically small antenna facilitated by a near-field resonant parasitic," *IEEE Antennas Wireless Propag. Lett.*, vol. 7, pp. 581–584, 2008.

[14] M. Makimoto and S. Yamashita, *Microwave Resonators and Filters for Wireless Communication: Theory, Design and Application*. Berlin, Germany: Springer, 2001.

[15] S. B. Cohn, "Parallel-coupled transmission-line-resonator filters," *IEEE Trans. Microw. Theory Techn.*, vol. MTT-6, no. 2, pp. 223–231, Apr. 1958.

[16] D. M. Pozar, *Microwave Engineering*, 4th ed. Hoboken, NJ, USA: Wiley, 2011.

[17] S. B. Cohn, "Shielded coupled-strip transmission line," *IEEE Trans. Microw. Theory Techn.*, vol. MTT-3, no. 5, pp. 29–38, Oct. 1955.

[18] J. Abraham, K. K. Aju John, and T. Mathew, "Microstrip antenna based on durer pentagon fractal patch for multiband wireless applications," in *Proc. Int. Conf. Commun. Embedded Syst. (ICICES)*, Feb. 2014, pp. 1–5.

[19] H. Omid and H. Oraizi, "Enhanced properties of a novel dual band shorted square patch with E-shaped slot for GSM/WLAN bands," in *Proc. IEEE Middle East Conf. Antennas Propag. (MECAP)*, Sep. 2016, pp. 1–4.

[20] N. Jin and Y. Rahmat-Samii, "Design of E-shaped dual-band and wide-band patch antennas using parallel PSO/FDTD algorithm," in *Proc. IEEE Antennas Propag. Soc. Int. Symp.*, Jul. 2005, pp. 37–40.

[21] N. J. Ramly, M. K. A. Rahim, M. E. Jalil, N. A. Samsuri, and R. Dewan, "Leaf-shaped dual band antenna for wearable application," in *Proc. Int. Symp. Antennas Propag. Conf.*, Dec. 2014, pp. 483–484.



HONGLIN ZHANG received the Ph.D. degree in t microelectronics and solid state electronics from the Nanjing University of Posts and Telecommunications. He is currently a Senior Engineer of the 54th Research Institute of China Electronic Technology Group Corporation (CETC54). His research interests include microwave and RF antenna, transceiver, and power amplifier.



TENG SUN received the M.S. degree in communication and information system from the 54th Research Institute of China Electronic Technology Group Corporation (CETC54), Shijiazhuang, China, in 2012. He is currently a Senior Engineer with the 54th Research Institute of CETC54. His research interest includes physical layer in wireless communications.



CHUNLEI YUAN received the M.S. degree, in 2012. He is currently with the 54th Research Institute of China Electronic Technology Group Corporation (CETC54), where he is also a Senior Engineer. His research interest includes wireless communications systems.



WENCHENG REN received the Ph.D. degree in communication and information system from the 54th Research Institute of China Electronic Technology Group Corporation (CETC54), Shijiazhuang, China, in 2015. He is currently a Senior Engineer with the 54th Research Institute of CETC54. His research interests include mobile and wireless communications.



DONG CHEN received the Ph.D. degree in electronic engineering from the Nanjing University of Posts and Telecommunications, Nanjing, China, in 2010. He has been an Assistant Professor in electromagnetic fields with the Nanjing University of Posts and Telecommunications, since 2014. His current research interests include the design of the microwave and RF antenna, transceiver, and power amplifier.

...